Journal of Hydroscience and Hydraulic Engineering
Vol. 19, No.1 May, 2001, 75-84

FIRST AND SECOND-ORDER FDS SCHEMES FOR FREE-SURFACE-PRESSURIZED FLOW SIMULATIONS

By

Akhilesh Kumar Jha, Juichiro Akiyama and Masaru Ura

Department of Civil Engineering, Kyushu Institute of Technology
Tobata, Kitakyushu 804-8550, Japan

SYNOPSIS

First and second-order flux-difference splitting schemes for free-surface flow simulations are combined with the Preissmann slot to simulate flows in a closed conduit, wherein the flow may change from free-surface to pressurized flow and vice versa. The models can simulate conduits with uniform cross-sections of arbitrary shape as well as with bed slope and bed friction. The models are verified with available experimental data on free-surface-pressurized flows for pipes and rectangular conduits. Thereafter, the models are tested against some exacting sample problems. It is demonstrated that the models yield very reasonable results in all the cases considered. A sensitivity analysis is performed for the size of the slot and useful conclusions are drawn from the study for the simulation of free-surface-pressurized flows.

INTRODUCTION

Flow in a closed conduit can be free-surface, pressurized or free-surface in some reaches while pressurized in others. Flows in a conduit with transitions from free-surface to pressurized flow, and vice versa, are called free-surface-pressurized flows. Such flows may occur in sewers, tailrace tunnel of a hydropower plant, tunnels of morning glory spillway, diversion tunnels, etc. Since free-surface and pressurized flows are governed by different equations, the simulation of free-surface-pressurized flows becomes problematic. However, a comparison of the governing equations for free-surface and pressurized flows reveals that the equations are identical if the depth of flow in the equation for free-surface flows is assumed equal to piezometric head in the case of pressurized flows (1).

Following this similarity, Priessmann developed a technique wherein a very narrow slot is assumed at the top of the conduit in such a way that it does not add to the wetted perimeter and its contribution to the flow area is negligible. This interesting concept facilitates computation of free-surface-pressurized flows by the shallow water equation alone.

Wiggert (2) computed free-surface-pressurized flow by a shock-fitting model and verified the numerical results with his experimental data. Baines et al.(3) did some preliminary works on the application of Roe's upwind TVD scheme to flows with steep waves in plant channels. They computed only one case of free-surface-pressurized flows and termed their outcome as inconclusive. Capart et al.(4) used the Pavia Flux Predictor scheme to compute the flow in sewer pipes and verified their model with experimental and field data. The model was found to accurately compute the considered cases. Garcia-Navarro et al.(5) presented an implicit method for computing the flow in channels and pipes. The model was reported to yield reasonable results for transient flows, particularly the flows with continuous or discontinuous steady states.

In this paper, flux-difference splitting schemes of Roe(6) and Lax-Wendroff, which have been well studied and found accurate in case of free-surface flow simulations (7,8), are combined with the Preissmann slot to simulate free-surface-pressurized flows. The models include bed slope and bed friction. The models are successfully verified against the experimental data of Capart et al.(4) and Wiggert (2). The models' applicability is tested with the problems of surge propagation in rectangular conduits. Finally, a sensitivity analysis is performed for the width of the slot with respect to the width of the conduit.

GOVERNING EQUATIONS

The governing equations for one-dimensional free-surface flows can be written as

$$\frac{\partial \mathbf{U}}{\partial t} + \frac{\partial \mathbf{E}}{\partial x} + \mathbf{S} = 0 \tag{1}$$

where **U** = vector of unknowns; **E** = flux vector; and **S** = vector containing source and sink terms. The vectors are given by

$$\mathbf{U} = \begin{pmatrix} A & uA \end{pmatrix}^T \tag{2a}$$

$$\mathbf{E} = \begin{pmatrix} uA & u^2A + gF_h \end{pmatrix}^T \tag{2b}$$

$$\mathbf{S} = \begin{pmatrix} 0 & -gA(S_o - S_f) \end{pmatrix}^T \tag{2c}$$

where A = flow area; u = flow velocity; g = acceleration due to gravity; S_o and S_f = bed and friction slopes; and F_h = hydrostatic pressure term defined as the first moment of the flow area about the free surface. The flux vector **E** is related to **U** through it's Jacobian **J** as

$$\mathbf{J} = \frac{\partial \mathbf{E}}{\partial \mathbf{U}} = \begin{bmatrix} 0 & 1 \\ gA/W(\eta) - u^2 & 2u \end{bmatrix} \tag{3}$$

where $W(\eta)$ = conduit width at a distance η from the conduit bottom. The governing equations are known to be hyperbolic, which means that **J** has a complete set of independent and real eigenvectors expressed as

$$\mathbf{e}^{1,2} = \begin{pmatrix} 1 \\ u \pm c \end{pmatrix} \tag{4}$$

$$c = \sqrt{\frac{gA}{W(h)}} \tag{5}$$

where c = celerity. The eigenvalues of **J** are given by

$$\lambda^{1,2} = u \pm c \tag{6}$$

Roe (6) constructed an approximate Jacobian in place of **J**, which makes the resulting scheme conservative. The approximate Jacobian uses following average value of velocities

$$u_{i\pm1/2} = \frac{A_{i+1}^{1/2} u_{i+1} + A_i^{1/2} u_i}{A_{i\pm1}^{1/2} + A_i^{1/2}} \tag{7}$$

and with the following definition of operators

$$\Delta(\bullet)_{i+1/2} = (\bullet)_{i+1} - (\bullet)_i \tag{8}$$

the average celerity is given as

$$c_{i\pm1/2}^2 = g \frac{\Delta(F_h)_{i\pm1/2}}{\Delta A_{i\pm1/2}} \tag{9}$$

FIRST-ORDER SCHEME

Roe's first-order accurate flux difference splitting scheme for one-dimensional transient free surface flows can be written as

$$\mathbf{U}_i^{t+1} = \mathbf{U}_i^t - \gamma\left[\mathbf{F}_{i+1/2}^t - \mathbf{F}_{i-1/2}^t\right] \tag{10}$$

where i and t = space and time indices, respectively; $\gamma = \Delta t/\Delta x$; Δt = time increment; and Δx = finite difference grid size in space. The treatment for the source term will be discussed later in the paper. All variables are computed at a known time level t, if not indicated otherwise. $\mathbf{F}_{i+1/2}$ and $\mathbf{F}_{i-1/2}$ are called numerical fluxes and are expressed as

$$\mathbf{F}_{i\pm1/2}^R = 0.5\left(\mathbf{E}_i + \mathbf{E}_{i\pm1}\right) - 0.5\sum_{k=1}^{2}\left|\lambda_{i\pm1/2}^k\right|\alpha_{i\pm1/2}^k\mathbf{e}_{i\pm1/2}^k \tag{11}$$

The superscript of $\mathbf{F}$ indicates numerical flux for Roe's first-order scheme. The wave strength, α is defined as

$$\alpha_{i\pm1/2}^{1,2} = \mathbf{e}_{i\pm1/2}^{-1}\Delta\mathbf{U}_{i\pm1/2} \tag{12}$$

$$\Delta\mathbf{U}_{i+1/2} = \mathbf{U}_{i+1} - \mathbf{U}_i \tag{13}$$

Roe's scheme is conservative and consistent with the governing equations. However, it violates energy inequality condition in case of a rarefaction wave. The most common remedy for this problem is to replace the modulus of λ in Eq.11 by a small positive quantity δ whenever the modulus of λ is less than δ. The value of δ can be set by trial but this paper uses the formula suggested by Harten and Hyman (9).

SECOND-ORDER SCHEME

The second-order accurate scheme is obtained by using the Lax-Wendroff numerical flux in Eq.10. Using the approximate Jacobian of Roe(6), the Lax-Wendroff numerical flux can be written as

$$\mathbf{F}_{i\pm1/2}^{LW} = 0.5\left(\mathbf{E}_i + \mathbf{E}_{i\pm1}\right) - 0.5\sum_{k=1}^{2}\left|\lambda_{i\pm1/2}^k\right|\alpha_{i\pm1/2}^k\mathbf{e}_{i\pm1/2}^k + 0.5\sum_{k=1}^{2}\varphi\tilde{\alpha}^k\left|\tilde{\lambda}^k\right|\left(1 - \gamma\left|\tilde{\lambda}^k\right|\right)\tilde{\mathbf{e}}^k \tag{14}$$

where ϕ = flux limiter, designed to prevent numerical oscillations due to the second-order of accuracy. The flux limiter is a non-linear function of

$$r_{i+1/2,j}^k = \left(\alpha_{i+1/2-\mathrm{sign}(\tilde{\lambda}_{i+1/2,j}^k),j}^k \Big/ \alpha_{i+1/2,j}^k\right) \tag{15}$$

We use the Van Albada limiter (10), which is expressed as

$$\varphi = (r + r^2)/(1 + r^2) \tag{16}$$

SOURCE TERM

The source term in the present study includes bed friction as well as bed slopes. The bed friction is computed by the Manning's formula as

$$S_f = \frac{Q|Q|n^2}{A^2R^{4/3}} \tag{17}$$

where n = Manning's roughness coefficient; Q= flow discharge; and R = hydraulic mean radius defined as R=A/P wherein P = wetted perimeter. In case of pressurized pipe flows, the following formulas can be used to compute flow depth/piezometric level, hydrostatic pressure term, and wetted perimeter. Let A_f = full cross-section area of the conduit, P_f= wetted perimeter at full flow, h_f = maximum height (diameter, d in case of a circular pipe) of the conduit, and b_s = width of the slot.

$$h = h_f + \frac{A - A_f}{b_s} \tag{18}$$

$$F_h = A_f\left(0.5h_f + \frac{A - A_f}{b_s}\right) + \frac{(A - A_f)^2}{2b_s} \tag{19}$$

$$P = P_f \tag{20}$$

The bed slope term contains the derivative of bed level with respect to the independent variable x. Following Roe (11), the bed slope term should be upwinded in the same way as the flux term **E**, the details of which are referred to Jha et al.(12).

NUMERICAL STABILITY

The scheme presented herein must satisfy the well known CFL condition for stability. Therefore, the new time increment is computed at the end of each calculation step by the following formula

$$\Delta t \le C_n \frac{\min(\Delta x)}{\max(u + c)} \tag{21}$$

where C_n= the Courant number.

NUMERICAL RESULTS

The models are first verified against available experimental data for free-surface-pressurized flows in circular pipes and in rectangular conduits. The case with a circular pipe is taken from Capart et al.(4). The experiments were conducted in a 12.74m long closed conduit of circular cross-sections connecting two tanks. The pipe had constant inside diameter of 0.145m but had three different longitudinal slopes in three sections as given below;

0.0m ≤ x ≤ 3.48m	0.01954 m/m
3.48m ≤ x ≤ 9.23m	0.01704 m/m
9.23m ≤ x ≤ 12.74m	0.01225 m/m

A constant discharge of 0.0042 m^3/s was provided from the upstream end throughout the experiment. This resulted in a supercritical flow throughout the pipe. The water level in the downstream tank was then raised by means of an outflow control weir, and a jump was eventually formed which traveled upstream in the pipe leaving pressurized flow behind. Just before the jump could reach the upstream end of the pipe, the water level in the downstream tank was drastically reduced which allowed the flow to return to its initial free-surface flow. The measured water level in the downstream tank is used as the downstream boundary condition in the numerical computations. The water/piezometric levels were recorded at seven points along the pipe: at x-0.325m, 1.135m, 3.06m, 5.505m, 6.835m and 7.6m. Other details of the experiment may be referred to Capart et al.(4).

The computations are carried out with Δx = 0.1m and the Courant number = 0.6. The slot width is specified as 10% of the pipe diameter. Figs.1 and 2 show the computed and recorded water surface profiles at 25s, 45s, 65s, 85s, 105s, 125s and 145s by Roe and Lax-Wendroff schemes, respectively. During these times, the jump forced by the raising of water level in the downstream tank advances upstream. Soon after 65s, the flow in the lower parts of the pipe becomes pressurized while in the rest of the pipe free-surface flow prevails.

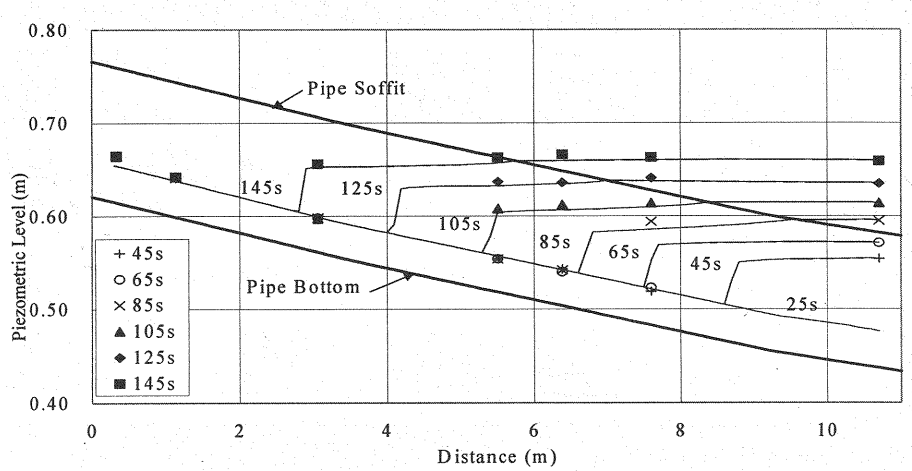

Fig.1 Surge moving upstream in a closed pipe by Roe Scheme.
Line – Computed, Symbol – Observed (Capart et al.(1997))

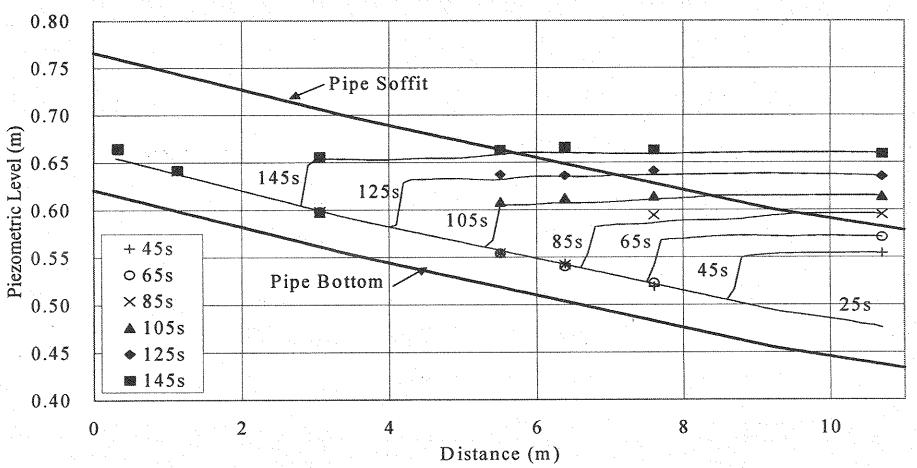

Fig.2 Surge moving upstream in a closed pipe by Lax-Wendroff Scheme.
Line – Computed, Symbol – Observed (Capart et al.(1997))

It can be seen from the figures that the models correctly compute the surge height and the celerity, both in the free-surface flow and in the pressurized flow regions. There is no noticeable difference between the results obtained by the Roe and the Lax-Wendroff schemes.

The water level in the downstream tank rises till 162s, when the surge is close to the inlet but yet to cause drowning of the inlet. Then the downstream water level is lowered suddenly. The surge begins to recede towards the downstream end and eventually the initial flow is restored. The water surface profiles during this depressurization phase are shown in Figs.3 and 4. The profile at 169s returns to fully free-surface flow and at 200s the initial flow profile has been fully restored. The computed profiles again compare very well with the observed data and there are again no significant differences between the results by the Roe and the Lax-Wendroff schemes. It may be noted that the experimental data used in this figure are different from Capart et al.(4). It has been confirmed through personal communications that the data given in Capart et al.(4) is partly in error. We have obtained the correct data from the first author for use in this paper.

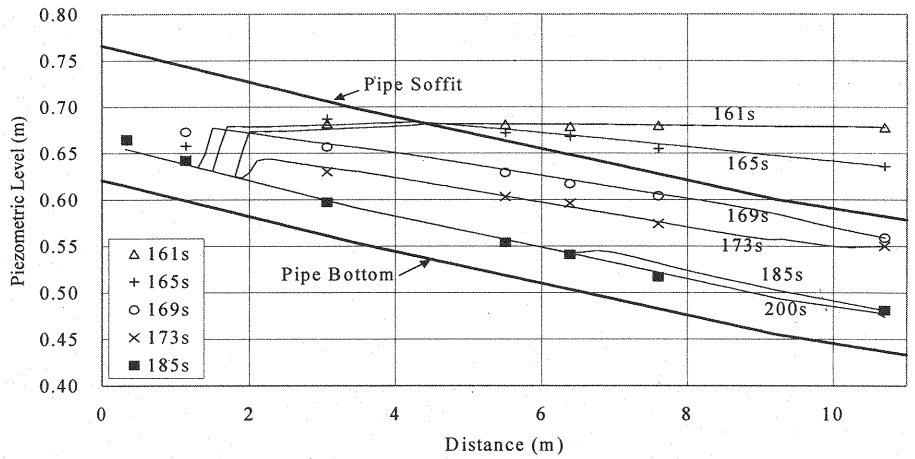

Fig.3 Surge receding downstream on lowering of water level in the downstream tank by Roe Scheme. Line – Computed, Symbol – Observed (Capart et al.(1997))

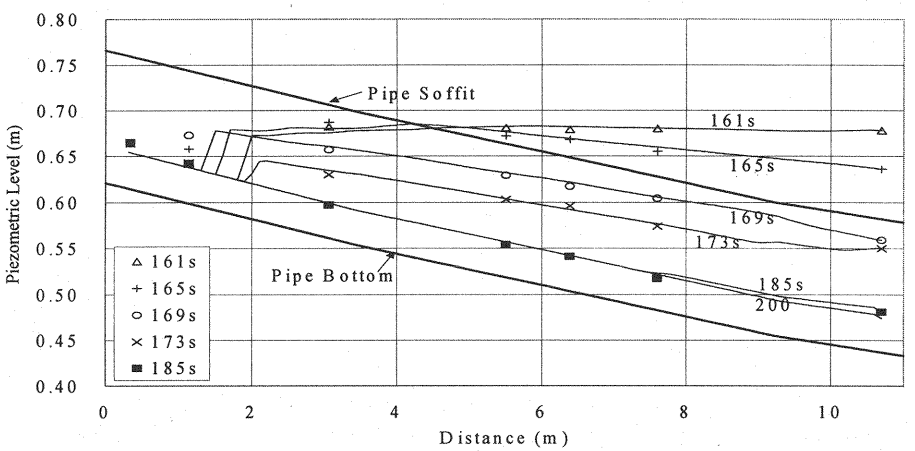

Fig.4 Surge receding downstream on lowering of water level in the downstream tank by Lax-Wendroff Scheme. Line – Computed, Symbol – Observed (Capart et al.(1997))

Fig.5 compares the computed and observed depth hydrographs at three locations along the pipe. The observed depth hydrographs were obtained by piezometers. The figure shows the computed results only by the Roe scheme for clarity. The model results compare reasonably with the recorded data in this figure as well.

The models are next verified with experimental data for a free-surface-pressurized flow in a rectangular conduit. The experimental data is taken from Wiggert (2). The data is measured for the flow in a 10 m long horizontal conduit of 0.51 m width and 0.148 m depth and Manning's roughness coefficient equals 0.012. The initial condition is 0.128 m deep still water throughout. The upstream boundary condition is specified by a depth hydrograph and the downstream boundary condition is a fixed water level. The recorded piezometric level at 3.5 m from the upstream end is used for comparison. The computations are carried out with $\Delta x = 0.1$ m and Courant number = 0.6. The results are shown in Fig.6. It can be seen that the computed results agree reasonably well with the observed data.

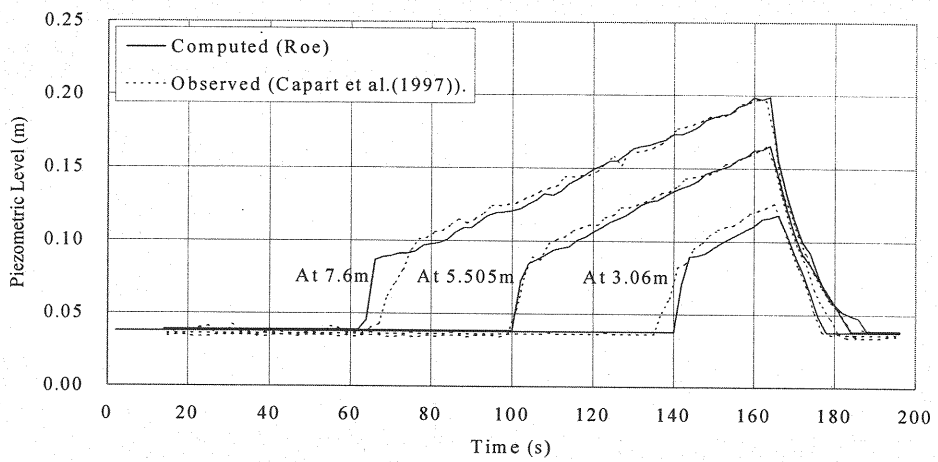

Fig.5 Plot of Piezometric levels at locations along the pipe

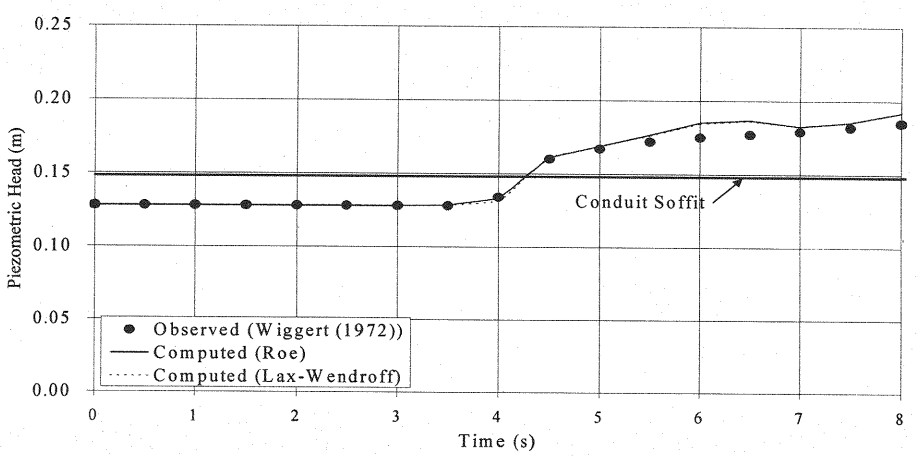

Fig.6 Surge propagation in a rectangular conduit. Line – Computed, Symbol – Observed

It is understood from these figures that the accuracy of results obtained by Roe's first-order accurate and Lax-Wendroff's second-order accurate schemes are almost identical. Hence, Roe's scheme may be preferred on the basis of its simplicity and less computation time. Therefore, the results by only Roe's scheme are presented in the following.

The model is now applied to conduits of rectangular cross-sections. The computations are carried out for the conduit of length 100m; the base width is assumed to be 1m. The Δx is 1m. The conduit lies horizontal and is frictionless. The computations for these cases are also carried out with a slot width equal to 10% of the conduit width.

In the first case, a uniform flow with the depth of 1m and the velocity 2 m/s flows through the conduit. At the start of the computation, a zero outflow condition, which simulates sudden closure of the conduit, is imposed at the downstream end. A surge is formed which travels upstream leaving still water behind. For the first run, it is assumed that the conduit is open at the top, so that the flow is never pressurized. Thereafter, the conduit is closed at a height of 1.5m. This causes the conduit to be pressurized from the downstream end as the surge is formed. The water surface profiles, for an open as well as a closed conduit, at 5s, 10s, 15s and 20s are shown in Fig.7.

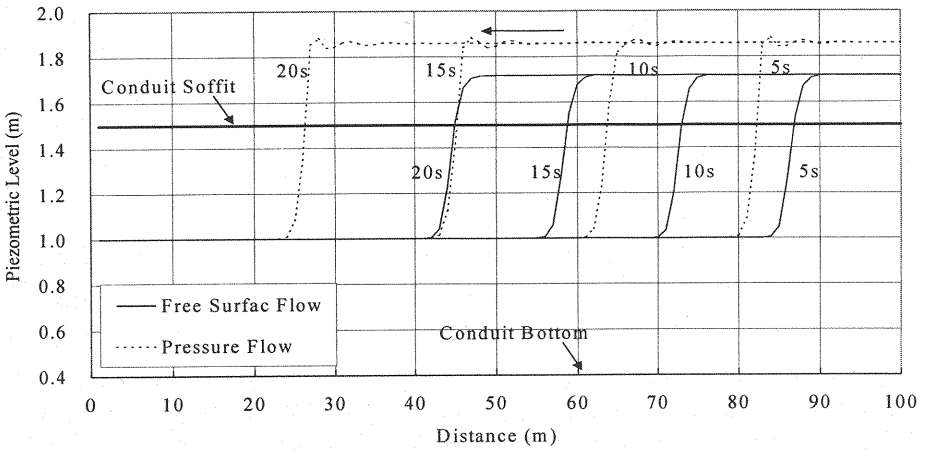

Fig.7 Reflected surge in a rectangular conduit

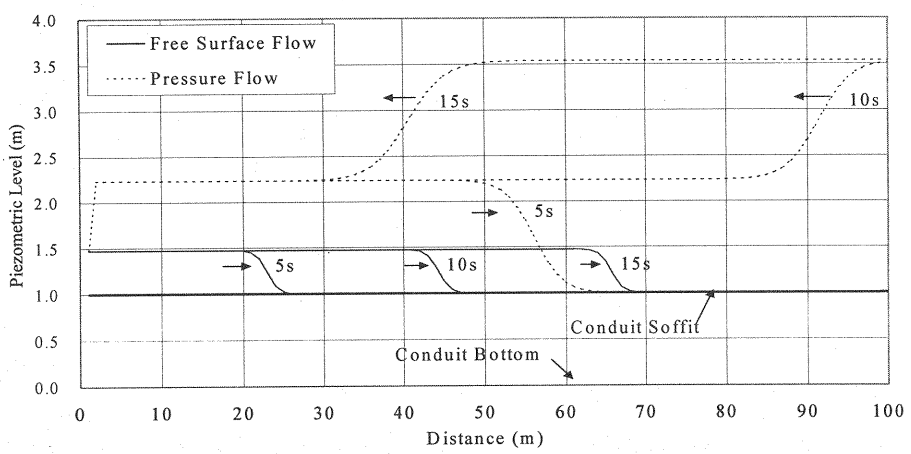

Fig.8 Surge entry and pressurization from upstream

It may be noted that for an open conduit, the analytical solution is also available. The numerical results perfectly agree with analytical solutions but the analytical solutions are not shown in the figure for the sake of clarity. As can be seen from Fig.4, the piezometric level rises higher than the case of a fully open conduit, which is expected. It is also noticed that at the interface between free-surface and pressurized flow zones, there are some oscillations.

In the second case, the conduit has 1m deep still water in the beginning and is closed at the downstream end. A constant discharge of 2.0 m^3/s is imposed at the upstream end, which creates a surge that travels downstream. As in the previous case, the result for open conduit is obtained first. Thereafter, the conduit is closed at a height of 1m. This generates pressurized flow with larger piezometric heads and faster celerity. The results are shown in Fig.8. It can be seen that the pressurized flow reaches the downstream end much faster than the case of fully free-surface flow, and at 10s and 15s the pressurized flow is travelling upstream after being reflected from the downstream end. The analytical solution for fully free-surface flow case is again not shown in the figure for the sake of clarity, but it is noted that the computed results very well agree with analytical solution for this case. The model reasonably computes pressurized flow and its reflection.

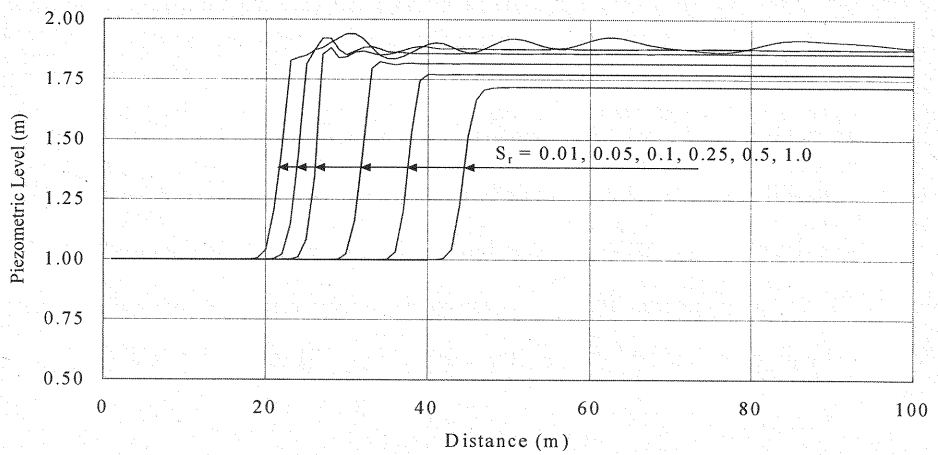

Fig.9 Sensitivity analysis for slot width

Finally, a sensitivity analysis is carried out to examine the effect of the slot size on the solution. The conduit is 1m wide and 1.5m high with 1m deep water flowing at 2 m/s as initial condition. The propagation of reflected surge following sudden closure at the downstream end is simulated with different ratio S_r of slot width b_s to conduit width b. Five values of the ratio of slot width to conduit width, S_r = 1.0, 0.5, 0.25, 0.1, 0.05, and 0.01, are used. The computed results at 20s are shown in Fig.9. It is seen from the figure that the piezometric levels do not change much when S_r is reduced further from 0.1 and the celerity also becomes only slightly faster. On the other hand, it is seen that the oscillations originating at the interface between free-surface and pressurized flow propagate throughout the surge and their amplitude increases considerably.

CONCLUSIONS

Roe and Lax-Wendroff flux-difference splitting schemes have been applied to free-surface-pressurized flows utilizing the concept of the Preissmann slot. The resulting models have been verified with experimental data for flows in pipes and rectangular conduits. The models' applicability has been tested with the applications to propagation and reflection of surge in rectangular conduits. The slot size used in the models is 10% of the width of the conduit. This value, besides giving accurate results, has been found to be most reasonable through a sensitivity analysis. This work shows that the first and second-order FDS schemes, with all their good features ascertained in case of free-surface flows, can also be a very good tool for simulating free-surface-pressurized flows.

ACKNOWLEDGMENT

This study was supported by the Grant-in-Aid for Science Research of the Ministry of Education and Culture, Japan under the Grant B(2), No.11450190.

REFERENCES

1. Chaudhry, M. H.: Applied Hydraulic Transients, Von Nostrand Reihhold, New York, 1979.
2. Wiggert, D. C.: Transient flow in free-surface-pressurized systems, J. of Hyd. Div., ASCE, Vol.98, No.HY1, pp.11-27, 1972.
3. Baines, M. J., Maffio, A. and Filippo, A. D.: Unsteady 1-D flows with steep waves in plant channels: the use of Roe's upwind TVD difference scheme, Advances in Water Resources, Vol.15, pp.89-94, 1992.
4. Capart, H., Sillen, X. and Zech, Y.: Numerical and experimental water transients in sewer pipes, J. of Hyd. Res., IAHR, Vol.35, No.5, pp.659-672, 1997.
5. Garcia-Navarro, P., Priestley, A. and Alcrudo, F.: An implicit method for water flow modelling in

channels and pipes, J. of Hyd. Res., IAHR, Vol.32, No.5, pp.721-742, 1994.
6. Roe, P. L.: Approximate Riemann solvers, parameter vectors and difference schemes, J. Comp. Physics, Vol.43, pp.357-372, 1981.
7. Jha, A. K., Akiyama, J. and Ura, M.: First- and second-order flux difference splitting schemes for dam-break problem, J. of Hyd. Engineering, ASCE., Vol.121, No.12, pp.877-884, 1995.
8. Glaister, P.: Approximate Riemann solutions of the shallow water equations, J. of Hyd. Res., IAHR., Vol.26, No.3, pp.293-306, 1988.
9. Harten , A. and Hymen, J. M.: Self adjusting grid method for one-dimensional hyperbolic conservation laws, J. Comp. Physics, Vol.50, pp.235-269, 1983.
10. Sweby, P. K.: High resolution schemes using flux limiters for hyperbolic conservation laws., SIAM J. Numer. Anal., Vol.21, pp.995-1101, 1984.
11. Roe, P. L.: Upwind differencing schemes for hyperbolic conservation laws with source terms 1st Int. Congress on Hyperbolic Problems, St. Etienne, 41-51, 1986.
12. Jha, A. K., Akiyama, J. and Ura, M.: Flux-difference splitting schemes for 2-D flood flows, J. of Hyd. Engineering, ASCE, Vol.126, No.1, pp.33-42, 2000.

APPENDIX - NOTATION

The following symbols are used in this paper :

A = cross-sectional area of flow;
b = conduit width;
b_s = width of slot;
C_n = Courant number;
c = celerity;
$\mathbf{E}$ = flux matrix;
$\mathbf{e}$ = matrix of eigenvectors of $\mathbf{J}$;
$\mathbf{F}$ = numerical flux;
F_h = hydrostatic pressure force;
g = acceleration due to gravity;
h = flow depth;
$\mathbf{J}$ = Jacobina of $\mathbf{E}$;
K = wave number;
n = Manning's roughness coefficient;
Q = flow discharge;
R = hydraulic mean radius;
r = ratio of wave strength for flux limiter;
$\mathbf{S}$ = matrix containing source terms;
S_f = friction slope;
S_o = bed slope
S_r = ratio of slot width, b_s to conduit width, b;
$\mathbf{U}$ = vector for flow variables;
u = flow velocity;
$W(\eta)$ = channel width at distance η from channel bottom;
Δt = time increment;
Δx = grid size in x-direction;
α = wave strength;
δ = small positive quantity;
ϕ = flux limiter;
γ = $\Delta t/\Delta x$;
η = integration variable indicating distance from channel bottom; and
λ = eigenvalues of $\mathbf{J}$.

(Received August 25, 2000 ; revised December 22, 2000)